Journal of Aeronautical
-Science and Engineering-
30th September 2018. Vol.15 No.1

August 30, 2018

Vortex Induced Vibration of Cold Water Pipe of OTEC

J.Koto,[a,b,*], Muhammad Zaki Prawira,[b]

[a)]*Ocean and Aerospace Research Institute, Indonesia*
[b)]*School of Mechanical Engineering, Universiti Teknologi Malaysia, Malaysia*

*Corresponding author: jaswar.koto@gmail.com , jaswar@utm.my

Paper History

Received: 25-July-2018
Received in revised form: 25-August-2018
Accepted: 30-August-2018

ABSTRACT

Ocean Thermal Energy Conversion (OTEC) is a process that can produce electricity by using the temperature difference between deep cold around 28 degree Celsius ocean water and warm tropical surface waters around 6 degree Celsius. Indonesia have many potential locations to build OTEC, among them is in Sumatera Utara, Bali, Flores Sea, Makassar Strait. The problem with pipes in the ocean is that as the ocean water flows past the pipe with a certain current velocity, a phenomenon called vortex-induced vibrations (VIV) might occur, potentially leading to very large oscillations. As the OTEC cold water pipe has unusual large diameter, the fluid will flow at unusual high Reynolds numbers. This paper investigates the effect flow past the pipe with different velocities and large diameters of pipe. The location is in Makassar strait and the velocity is obtained by data from previous researcher based on deep water is 0.8 m/s, 0.62 m/s, 0.46 m/s , 0.35 m/s , 0.28 m/s. The large diameter of pipe is obtained used OTEC Pro Simulation based on population in Karampuang Island at the Makassar strait is 4m and 3m diameter of pipe. The result obtained from numerical simulation used ANSYS FLUENT.

KEY WORDS: *Vortex Induced Vibration; OTEC; Cold Water Pipe; ANSYS.*

NOMENCLATURE

OTEC	Ocean Thermal Energy Conversion
CFD	Computational Fluid Dynamic
VIV	Vortex Induced Vibrations
CWP	Cold Water Pipe
FFT	Fast Fourier Transform

1.0 INTRODUCTION

Vortex Induced Vibration is a phenomenon where objects such as cylinder interact with moving fluid through it. When an object is immersed in moving water, it will experience a phenomenon where the sea currents caused the object to be excited by forces that caused by vortex shedding [1]. The vortex shedding is an unsteady flow that occurred in special flow velocities depend on size shape of the object. The vortex shed occurred at the back of the body and separated periodically from each side of the body causing the time varying different pressure around the object explained that the vortex shed are not occurred symmetrically. This unsymmetrical vortex shedding cause the different lift force around the object resulting vibration of the object in both parallel and perpendicular to the moving flow cause the cylinder body to move. The lock-in phenomena is associates with this vortex-induced vibration since it related with Eigen frequency of the riser and also frequency of the sea current.

The vortex-induced vibration is known as self-exciting, self-regulating, self-limiting highly phenomenon that received extensive attention in this oil and gas industry due to the flow-structure-interaction problem [2]. This phenomenon commonly are excited by vortex shedding due to external load that is sea currents as the riser is experiencing sea currents in deep-water. The vortex-induced vibration also influenced by a large number of parameters including mass ratio, structure stiffness, damping, surface roughness and the most important parameters for this vortex-induced vibration are Reynolds number, Strouhal number, and reduced velocity [3].

Vortex Induced Vibration (VIV) becomes one of the problems that concern in marine application such as Cold Water Pipe (CWP) which is designed to Ocean Thermal Energy Conversion (OTEC) from sea bed [4]. The CWP systems may have potential in experiencing a highly level of fatigue damage in

Published by International Society of Ocean, Mechanical and Aerospace Scientists and Engineers, www.isomase.org., ISSN: 2442-6407

ISOMAse
International Society of Ocean, Mechanical and Aerospace Scientists and Engineers
Journal of Aeronautical
-Science and Engineering-
30th September 2018. Vol.15 No.1

August 30, 2018

a relatively period of time due to exposure of the CWP to harsh current environments because of Vortex Induced Vibration

OTEC can be done effectively and on a large scale to provide a source of renewable energy that is needed to cover a wide range of energy issues. Floating Ocean Thermal Energy Conversion (FOTEC) system usually consist an up to 500 m long Cold Water Pipe and used large diameter.

Indonesia is the tropical oceans country, approximately defined by latitudes less than 20 degrees, may be thought of as enormous passive solar collectors. Indonesia has 77 % of total area covered by the ocean. Therefore, renewable energy from OTEC is potential for a power source for small islands to larger islands in Indonesia. The potential location for OTEC is South Kalimantan, East Kalimantan, Makassar Strait, Timur Strait, and Morotai Island [5-13].

Wind, sea current and ocean surface waves is a concern for in floating ocean thermal energy conversion (OTEC) system design. Important to study the addiction of the cold water pipe (CWP) on the effect of drag amplification due to vortex induced vibrations, relative velocity of the flow around the pipe [14, 15]. This paper focuses on flow around cylinder with condition environment in Makassar Strait use computational fluid dynamics (CFD).

2.0 GOVERNANCE EQUATION

2.1 Drag (F_D) and Lift (F_L)Forces

Friction can also contribute to this force. These forces can be divided into two types which are lift for and drag force. As mentioned in the previous section, shedding vortices will cause irregular and periodic changed pressure distribution that contributes to the external and resultant force on the body of cylindrical structure [6]. Lift force moves in cross-flow direction while drag force moves in in-line direction as shown in figure 1.

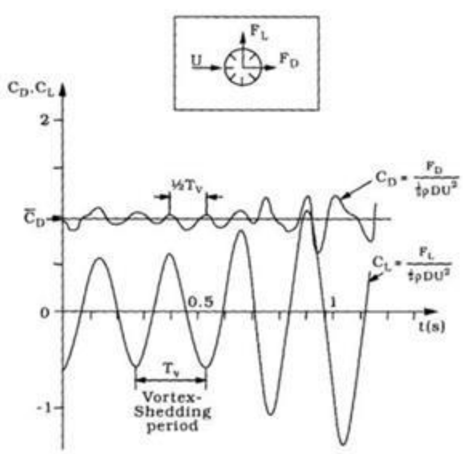

Figure 1: Oscillating drag and lift forces traces, adapted from Sumer [16]

Drag force (F_D) and Lift force (F_L) are formulated:

$$F_D = C_D \frac{1}{2} \rho D L U^2 \quad (1)$$

$$F_L = C_L \frac{1}{2} \rho D L U^2 \quad (2)$$

Where: C_D is drag coefficient, C_L is lift coefficient, ρ is Fluid density, L is Length of cylinder, D is Cylinder diameter and U is flow velocity,

2.2 Strouhal Number (S_t)

The Strouhal Number (S_t) is proportional to the shedding frequency of the fluid, and given as:

$$S_t = \frac{f_s \cdot L}{U} \quad (3)$$

Where; f_s is the frequency of vortex shedding, L is the characteristic length (for example hydraulic diameter, or chord length) and U is the flow velocity.

Avoiding resonance on riser would be an efficient way of avoiding the VIV phenomenon. This means that the reduced velocity (U_r) is kept lower than 1 (Blevins, 1994). Reduced velocity (U_r) can be expressed as

$$U_r = \frac{U}{f_n L} < 1 \quad (4)$$

Where; f_n is the natural frequency which can be expressed as:

$$f_n = \frac{1}{2\pi} \sqrt{\frac{k}{m + m_a}} \quad (5)$$

Where; m is mass of cylinder, m_a is added mass, k is riser stiffness. Increasing the stiffness of the structure will increase the natural frequency of the structure, thus reducing the reduced velocity.

The mass ratio can be expressed as

$$m^+ = \frac{m}{\rho \pi L \frac{D^2}{4}} \quad (6)$$

The riser stiffness can be written as

$$k = \mathrm{EI} \quad (7)$$

Where; E is Modulus of Elasticity, I is the second moment of area, about an axis in the plane of the cross section through the centroid.

$$I = \pi \left(D_o^4 - D_i^4\right) / 64$$

D_o is outer diameter of pipe and D_i is inner diameter of pipe

3.0 INPUT DATA AND SIMULATION

3.1 Sea Current Profiles

Karampuang Island is an island located in Karampuang Village, Makasar Strait, West Sulawesi Province, The area of Karampuang Island is 6.37 km2 with a population around 5000 people and system of OTEC used closed cycle.

JAse | Received: 25-July-2018 | Accepted: 30-August-2018 | [(15) 1: 1-9]
Published by International Society of Ocean, Mechanical and Aerospace Scientists and Engineers, www.isomase.org., ISSN: 2442-6407

Journal of Aeronautical
-Science and Engineering-
30th September 2018. Vol.15 No.1

Sea water circulation at the surface layer at the Makasar Strait is strongly influenced by monsoon wind in which the pattern circulation changes according to wind patterns. During the west monsoon currents the surface moves in the main direction from west to east and in season east going the opposite [17]. Geographical position also affects the movement of surface currents in the waters of the Selat Makassar.

In the Selat Makasar the sea current flows throughout the year to the south and with moderate speed. The velocity profile as shown Figure 2.a-d displays a distinct thermocline maximum ($V - Max$) between 0 to 300 m [18, 19]. The profile varies with season: the greater $V - Max$ during July-August-September (JAS) profile during Southeast monsoon, relative to the January-February-March (JFM) profile during Northwest monsoon.

The JAS and JFM profiles reverse their relative position at depths below 220 db, indicating a deeper reaching Makassar throughflow during the Northwest monsoon. The time series section of the along-axis current, right further displays the depth dependence of the $V - Max$, with a tendency for the higher speeds as the v-max shallows. The $V - Max$ deepens during the northwest monsoon, February-March 2004, March-April 2005 and February-April 2006; with the shallowest v-max during the southeast monsoon, July-September 2004, 2005 and 2006. The thermocline v-max displays a semi-annual fluctuation, with highest values within the middle to latter stage of each monsoon: February-April 2004, July-September 2004, March-April 2005, August-September 2005, February-March 2006, June-September 2006. The strong southward speeds in 2006 stand out as an anomaly, lacking the May/June throughflow relaxation as observed in the two prior years. The period of sustained throughflow begins rather abruptly in early February 2006, spanning a wide swath of depths, from the sea surface to well below the thermocline.

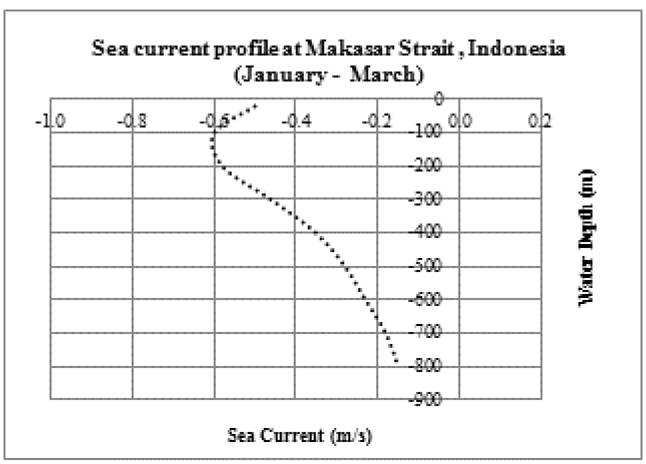

Figure 2.a: Sea current at Selat Makasar, Indonesia from January to March during Northwest monsoon [17].

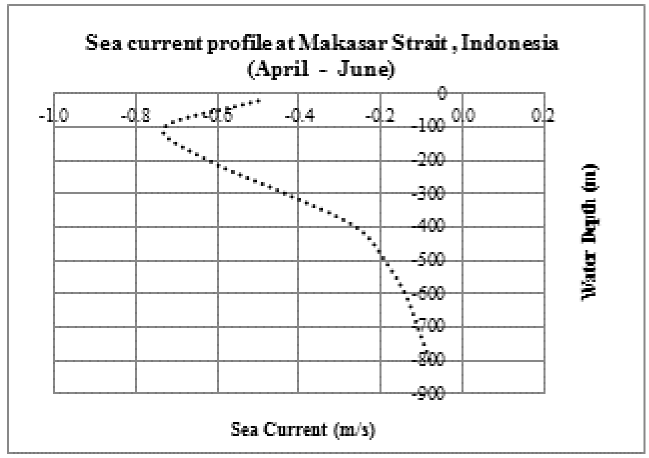

Figure 2.b: Sea current at Selat Makasar, Indonesia from April to June [17].

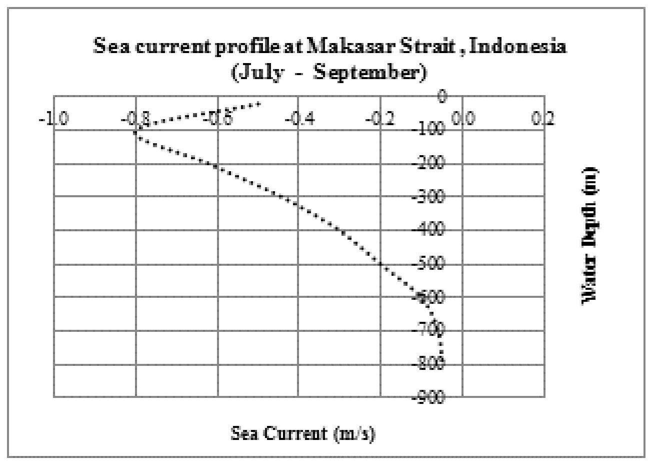

Figure 2.c: Sea current at Selat Makasar, Indonesia from July to September during Southeast monsoon [17].

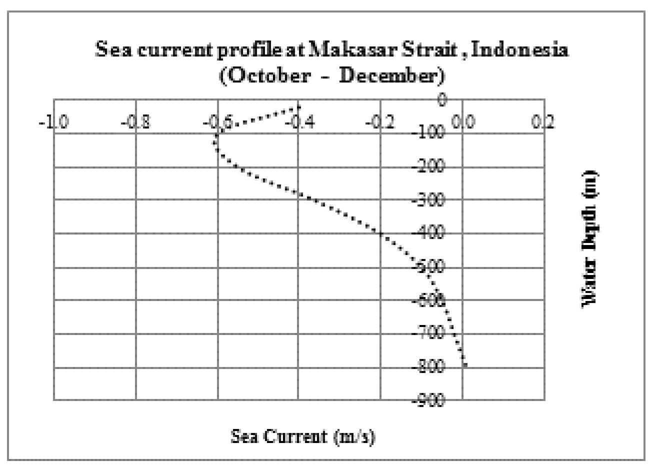

Figure 2.d: Sea current at Selat Makasar, Indonesia from October to December [17].

3.2 Cold Water Pipe Specification

JAse | Received: 25-July-2018 | Accepted: 30-August-2018 | [(15) 1: 1-9]
Published by International Society of Ocean, Mechanical and Aerospace Scientists and Engineers, www.isomase.org., ISSN: 2442-6407

ISOMAse
International Society of Ocean, Mechanical and Aerospace Scientists and Engineers

Journal of Aeronautical
-Science and Engineering-
30th September 2018. Vol.15 No.1

August 30, 2018

The diameter of the pipe calculated based on total energy required of OTEC and cold water flow rate. In this study is calculated by software OTEC Pro Simulation as shown in Figure 3. Table 1, Table 2 and Table 3 show the parameter data.

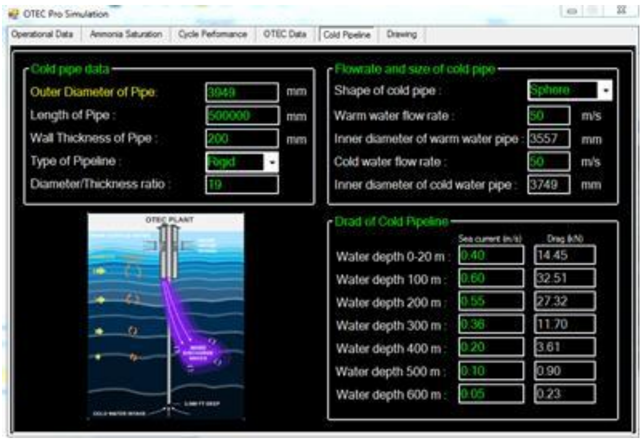

Figure 3: Meshing configuration

Table 1: CWP specifications

Properties of CWP	Dimensions
CWP for flow rate 100 m/s	
Outer diameter of CWP	3.00 m
Inner diameter of CWP	2.65 m
Wall Thickness of CWP	0.30 m
CWP for flow rate 50 m/s	
Outer diameter of CWP	4.00 m
Inner diameter of CWP	3.75 m
Wall Thickness of CWP	0.20 m

For modeling cold water pipe will performed with Design Modeler Geometry and for performance analysis will performed with ANSYS fluent with turbulent model used K-ε Realizable and Pressure-Velocity Coupling Scheme used PISO.

3.3 Solution Domain

The solution domain is the abstract environment where the solution is calculated. The shape of the solution domain can be circular or rectangular depending on the characteristics of the solution. Generally, many simulations use a rectangular box shape as the solution domain. The selected solution domain is L = 40D times D = 17D and the center of the cylinder is 10D at x-axis and 8.5D at y-axis. In the selection of solution domain size and shape, it is compulsory to consider the optimum size. If the size of the domain is too small, less time is needed for the solution to be solved in compare to the large scale of solution domain.

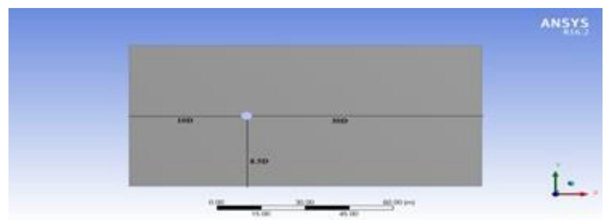

Figure 4: Solution Domain in Design Modeler

3.4 Meshing Configuration

The meshing configuration is clear after solution domain is created. The term meshing and grid generation is interchangeable and has similar literal meaning.

Table 2: R_e for Diameter of pipe in 3m

Sea Current Velocity, U (m/s)	Reynolds Number, Re	Temperature (ºc)	viscosity	Sea Current density (kg/m^3)	Water Depth (m)
0.80	2.37E+05	21.5	1.04E-03	1024	100
0.62	1.61E+06	16.0	1.18E-03	1025	200
0.46	1.05E+06	11.0	1.35E-03	1026	300
0.35	7.29E+05	8.0	1.48E-03	1027	400
0.28	5.49E+05	6.0	1.57E-03	1027	500

Table 3: R_e for Diameter of pipe in 4m

Sea Current Velocity, U (m/s)	Reynolds Number, Re	Temperature (ºc)	viscosity	Sea Current density (kg/m^3)	Water Depth (m)
0.80	3.16E+06	21.5	1.04E-03	1024	100
0.62	2.15E+06	16.0	1.18E-03	1025	200
0.46	1.40E+06	11.0	1.35E-03	1026	300
0.35	9.71E+05	8.0	1.48E-03	1027	400
0.28	7.33E+05	6.0	1.57E-03	1027	500

JAse | Received: 25-July-2018 | Accepted: 30-August-2018 | [(15) 1: 1-9]
Published by International Society of Ocean, Mechanical and Aerospace Scientists and Engineers, www.isomase.org., ISSN: 2442-6407

Journal of Aeronautical
-Science and Engineering-
30th September 2018. Vol.15 No.1

August 30, 2018

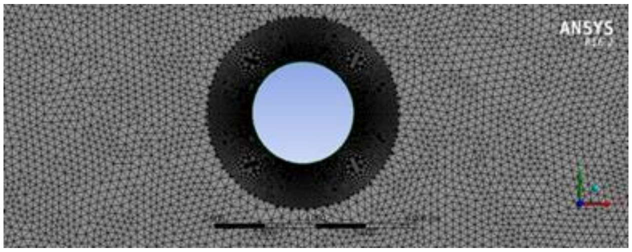

Figure 5: Meshing configuration used ANSYS Fluent.

Table below show statistic meshing in ANSYS Fluent based on current study.

Table 4: Details of meshing configuration

Statistics	Description
Number of Nodes	120348
Number of Elements	213840
Solution Method	Triangular Method

3.5 Boundary Condition

Boundary condition, as mentioned previously is the process where variable flow information is specified. Boundary conditions can be classified as inlet, outlet, wall, symmetry, periodic and axis boundaries. Inlet boundary is the condition that allows the flow into the solution domain. The parameters include pressure, velocity and mass flow inlets. The outlet is the condition that allows the flow out of the solution domain.

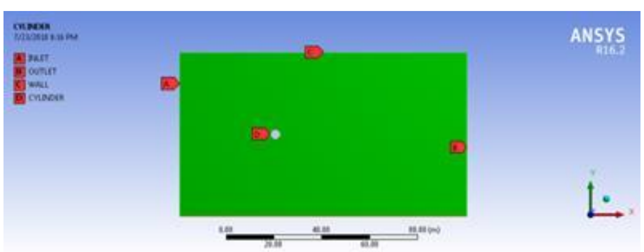

Figure 6: Boundary condition defined in current studies.

3.6 Validation

This section will describe the validation of results obtained from simulation previously. In current studies, the method of validation is by comparing the results with Strouhal Number (St).

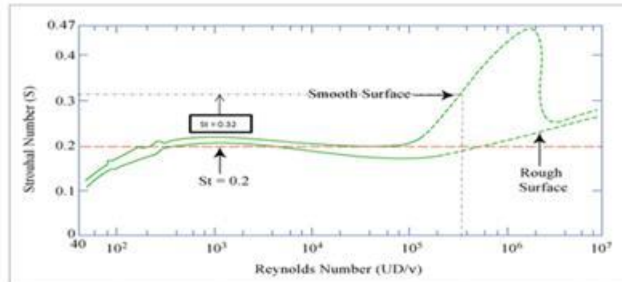

Figure 7: Variation in vortex pattern based on Reynolds number (R_e) [4].

From Figure 7, Lienhard specifies the relationship between Strouhal number ($\boldsymbol{S_t}$) and Reynolds number (R_e) [18]. The Reynolds number (R_e) is from the range R_e = 0 until 107. In current studies, Reynolds number was taken from 100000 until 300000. As per shown in Figure 6, the Strouhal number (St) should be around 0.32 for (R_e) 549477.707 at smooth surface. The Fast Fourier Transform (FFT) is implemented to calculate (St).

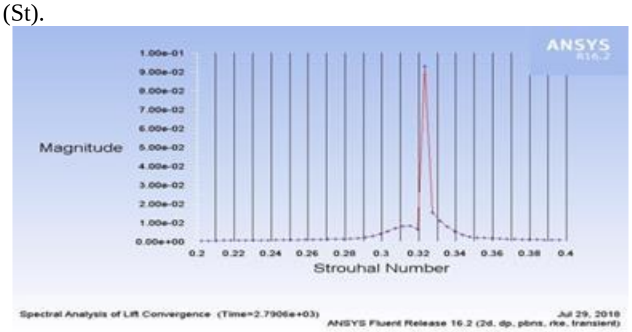

Figure 8: FFT Plot at Re = 549477.707

4.0 RESULTS AND ANALYSIS

4.1 Drag (C_d), Lift (C_l) , and Shedding Frequency (F_v)

From figure 9 the higher Cd for diameter 4m at 500 m is 1.24 and lower is at 100m Cd is 0.904 and the higher Cd for diameter 3m at 500 m is 0.825 and lower is at 100m Cd is 0.69. Because at 500 m the force is bigger so can increase friction Drag and also The Area is mean Diameter can increase for in-line direction.

From Figure 10 the higher C_l for diameter 4m at R_e 3.16E+06 in 100 m is 0.181 and lower is at 100 m C_l is 0.04 .The higher C_l for diameter 3m at R_e 2.37E+05 in 100 m is 0.121 and lower is at 500m C_l is 0.03.

The shedding frequency is obtained from lift coefficient (C_l) history and The Fast Fourier Transform (FFT) is implemented to calculate the frequencies spectrum of f_v. From figure 5.22 is obtained the high Shedding Frequency F_v is at at Re 3.16E+06 in 100 m for diameter 4m is 0.11 Hz. the high Shedding Frequency F_v is at at Re 3.16E+06 in 100 m for diameter 3m is 0.072 Hz.

JAse | Received: 25-July-2018 | Accepted: 30-August-2018 | [(15) 1: 1-9]
Published by International Society of Ocean, Mechanical and Aerospace Scientists and Engineers, www.isomase.org., ISSN: 2442-6407

Journal of Aeronautical
-Science and Engineering-
30th September 2018. Vol.15 No.1

August 30, 2018

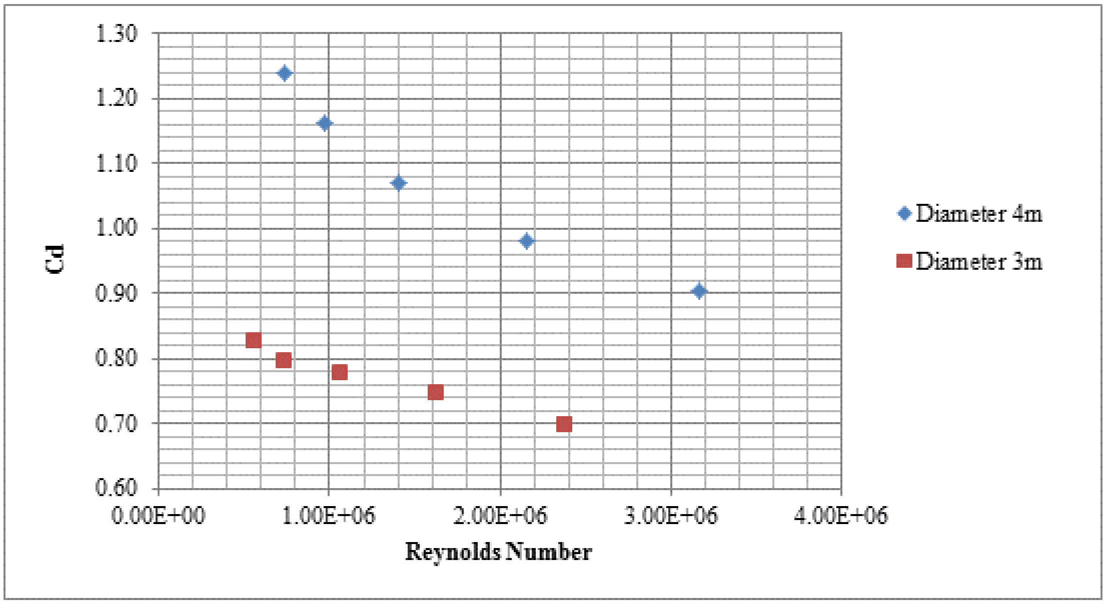

Figure 9: Comparison of C_d

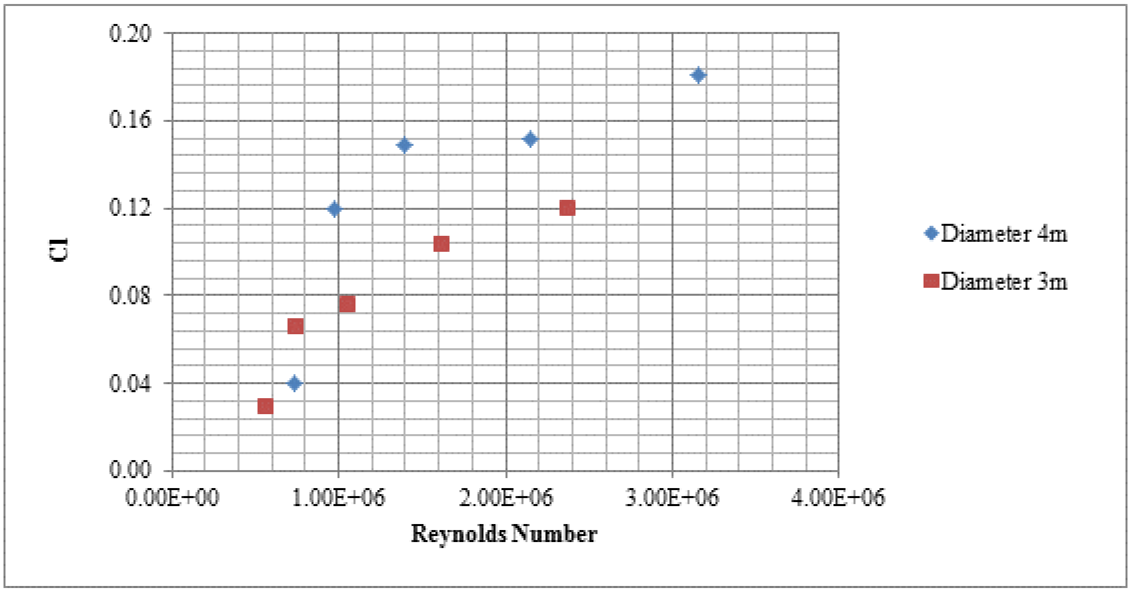

Figure 10: Comparison of C_l

JAse | Received: 25-July-2018 | Accepted: 30-August-2018 | [(15) 1: 1-9]
Published by International Society of Ocean, Mechanical and Aerospace Scientists and Engineers, www.isomase.org., ISSN: 2442-6407

ISOMAse
International Society of Ocean, Mechanical and Aerospace Scientists and Engineers

Journal of Aeronautical
-Science and Engineering-
30th September 2018. Vol.15 No.1

August 30, 2018

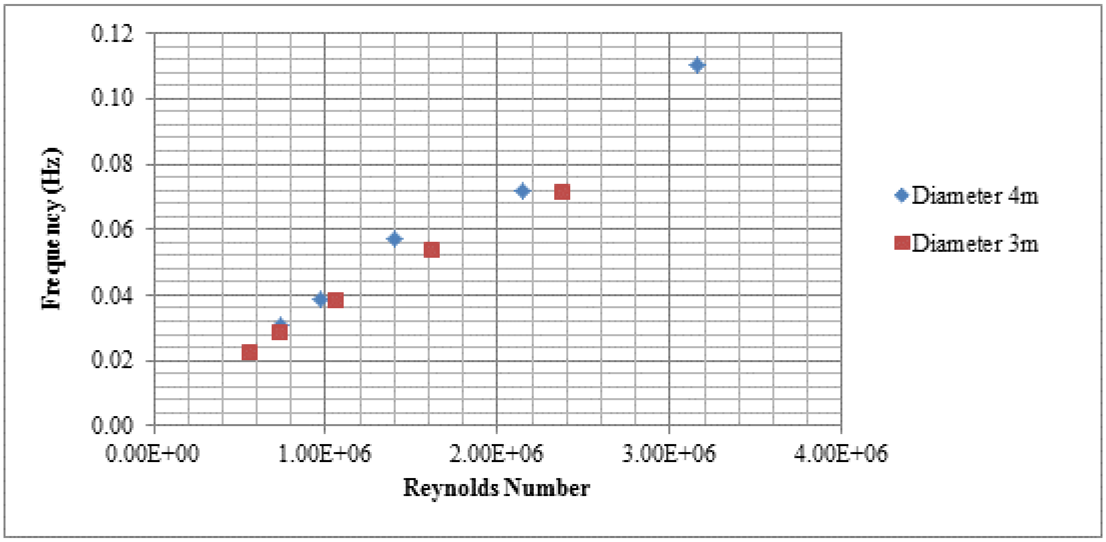

Figure 11: Comparison of F_v

4.2 Flow Pattern of Turbulent Velocity and Velocity Contour

The Turbulent Velocity and Velocity Contour is compared to see the relationship of flow between Diameter 3m and 4m and also velocity at 0.8 m/s in deep 100 m, 0.62 m/s in deep 200 m, 0.46 m/s in deep 300 m, 0.35 m/s in deep 400 m, 0.28 m/s in deep 500 m. The Turbulent Velocity and Velocity Contour as shown in Table 5 is taken at global time lapse to obtain the result where the changes in the contour at unsteady state. We can see a higher turbulence at 0.8 m / s at a depth of 100m and the lower the velocity, the turbulent becomes smaller.

Deep	Diameter 3m Turbulent Velocity & Velocity Contours	Diameter 4m Turbulent Velocity & Velocity Contours
100 m	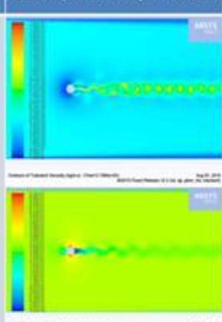	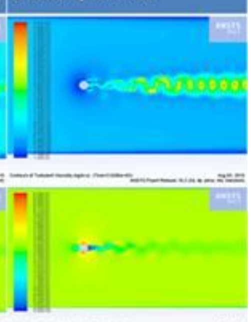

Deep	Diameter 3m Turbulent Velocity & Velocity Contours	Diameter 4m Turbulent Velocity & Velocity Contours
200 m	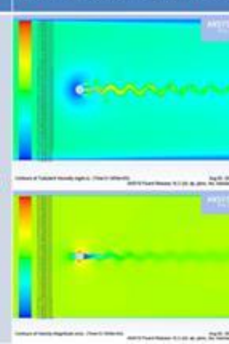	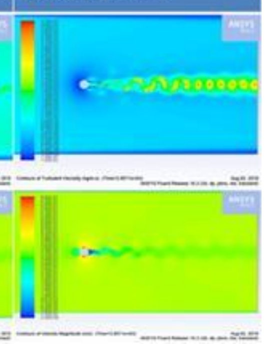

Deep	Diameter 3m Turbulent Velocity & Velocity Contours	Diameter 4m Turbulent Velocity & Velocity Contours
300	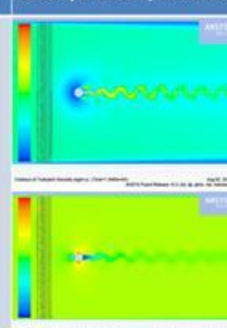	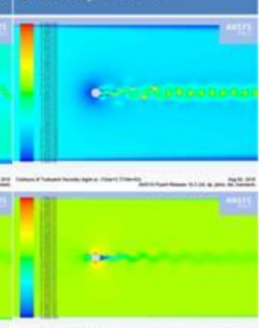

JAse | Received: 25-July-2018 | Accepted: 30-August-2018 | [(15) 1: 1-9]
Published by International Society of Ocean, Mechanical and Aerospace Scientists and Engineers, www.isomase.org., ISSN: 2442-6407

ISOMAse
International Society of Ocean, Mechanical and Aerospace Scientists and Engineers

Journal of Aeronautical
-Science and Engineering-
30th September 2018. Vol.15 No.1

August 30, 2018

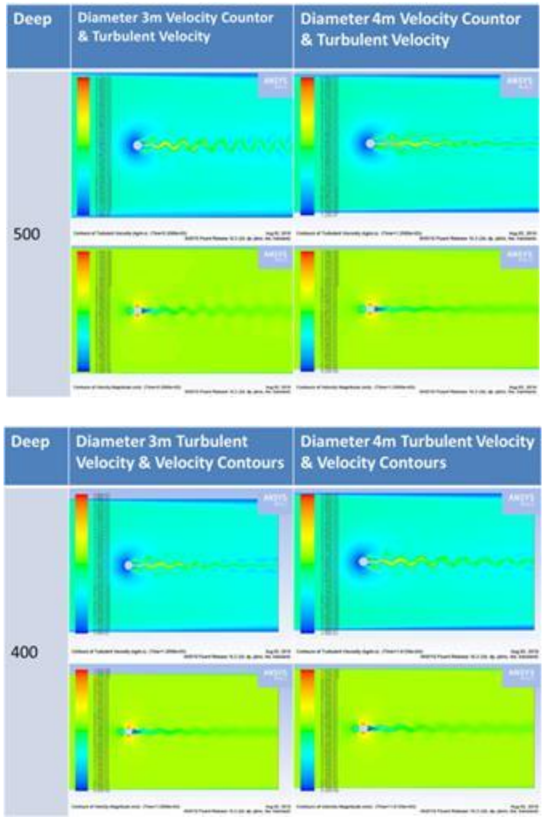

Table 5: Flow Pattern of Turbulent Velocity and Velocity Contour

5.0 CONCLUSION AND RECOMMENDATION

The main purpose of this research study is to determine suitable diameter of cold water pipes for OTEC system in Makassar Strait, Indonesia and to analyze vortex induced vibration of the selected cold water pipes using different Velocity & diameters.

The simulation is done to study the analyze Flow past the cylinder with different velocity and diameter. By Using ANSYS FLUENT, the Reynolds number was performed on cylinder.

Based on the result obtained from the simulation, the suitable diameter for OTEC in Karampuang Island, Makassar strait is 4m and 3m based on flow rate and energy requirement 0.005 MW for 5000 people with the Closed Cycle system. The In-line decreases with the increase of Re otherwise Cross- flow is increase with the increase Re and also increase the shedding frequency. The high vibration is in diameter 4m at Re 3.16E+06 in deep 100m is 0.11 Hz

From the simulation and results outcome, there is an improvement that can be practiced in future work for more accurate and better findings in the analysis:

a. To conduct simulation 3D on the effect of other parameters such as diameter and Material aspect of VIV amplification.
b. To conduct dynamic solution and UDF (Unit Defined Function) to obtain better observation on the amplification of vibration.
c. To conduct the experimental analysis for more reliable outcome.

ACKNOWLEDGMENT

The authors would like to thank Universiti Teknologi Malaysia and Ocean and Aerospace Research Institute, Indonesia for supporting this study.

REFERENCE

1. Jaswar, M. K. R. A. Razak and C. L. Siow, 2013. Vortex-Induced Vibration of Riser, *International Conference on Marine Safety and Environment*, Johor Bahru, Malaysia.
2. Jaswar Koto, et.al, 2013, Vortex-Induced Vibration of Riser Caused by External Load., *The 12th Asian International Conference on Fluid Machinery*, Yogyakarta, Indonesia.
3. Jaswar Koto, Abdul Khair Junaidi, 2014, *Analysis of Vortex-Induced Vibration of Riser using Spalart-Almaras Model*, Jurnal Teknologi, Vol 69, No 7, pp. 69:7 (2014) 9–15.
4. Muhammad Zaki Prawira, Jaswar Koto, 2018, Vortex Induced Vibration on Cold Water Pipe of OTEC, *The 11th International Conference on Marine Technology MARTEC 2018*, Offshore Engineering, pp.33-41.
5. J. Koto, Adek Tasri, Insannul Kamil, Taufik, Dodi Sofyan Arief, Efiafrizal, 2017, *Sea Temperatures Profiles for Ocean Thermal Energy Conversion in Siberut-Mentawai, Sumatera Barat, Indonesia*, Journal of Subsea and Offshore -science and engineering-, Vol.11, pp.7-13.
6. Jaswar Koto, 2016, *Potential of Ocean Thermal Energy Conversion in Indonesia*, International Journal of Environmental Research & Clean Energy, Vol.4, pp.1-7.
7. Jaswar Koto, Adek Tasri, Insannul Kamil, Dodi Sofyan Arief, 2017, *Potential of Solar-Wind-Ocean Thermal Energy Conversion in Indonesia*, Ocean and Aerospace Research Institute, Second Edition, March.
8. Jaswar Koto, Ridho Bela Negara, 2016, *Preliminary Study on Ocean Thermal Energy Conversion in Siberut Island, West Sumatera, Indonesia*, Journal of Aeronautical -science and engineering-, Vol.6, pp.1-7.
9. Jaswar Koto, Ridho Bela Negara, 2016, *Study on Ocean Thermal Energy Conversion in Morotai Island, North Maluku, Indonesia*, Journal of Aeronautical -science and engineering-, Vol.7, pp.1-7.
10. Jaswar Koto, Ridho Bela Negara, 2016, *Study on Ocean Thermal Energy Conversion in Seram Island, Maluku, Indonesia*, Journal of Aeronautical -science and engineering-, Vol.8, pp.1-7,
11. Jaswar Koto, Ridho Bela Negara, 2017, *Potential of 100 kW of Ocean Thermal Energy Conversion in Karangkelong, Sulawesi Utara, Indonesia*, International Journal of Environmental Research & Clean Energy, Vol.5, pp.1-10.
12. Jaswar Koto, 2017, *Potential of Solar-Wind-Ocean Thermal*

Energy Conversion in Indonesia, Ocean and Aerospace Research Institute, March.

13. Mohd Fahmie, J.Koto, Nofrizal, A.Edu, U.Zulkarnain, 2018, *Ocean Thermal Energy Conversion in Layang-Layang and Kuala Baram, Malaysia*, International Journal of Environmental Research & Clean Energy, Vol.11 No.1, pp.12-21.
14. Jiang, L. (2013). *Deepwater Internal Wave Study and Application*, M Sc Thesis, University of Texas.
15. Adi Maimun, M. Mobassher, Yasser, M. Ahmad. 2012. *Fundamentals of Vortex Induced Vibration Analysis of Marine Riser*, Offshore Mechanics and Hydrodynamics, Mechanical–Marine Technology, University Technology Malaysia, Johor, Malaysia.
16. Lienhard, I. H. (1966). *Synopsis of lift, drag and vortex frequency data for rigid circular cylinders*, Washington: Washington State University.
17. Zaki Prawira, J. Koto, Dodi Sofyan Arief, Delyuzar Ilahude, Adek Tasri, Insannul Kamil, Taufik, 2018, *Cooling Pipe of Offshore Ocean Thermal Energy Conversion in Selat Makassar, Indonesia*, International Journal of Environmental Research & Clean Energy, Vol.10 (1), pp.1 - 61.
18. Gordon, A. L., R. D. Susanto, A. Ffield, B. A. Huber, W. Pranowo, and S. Wirasantosa (2008), *Makassar Strait throughflow, 2004 to 2006, Geophys*. Res. Lett., 35
19. Susanto, R. D., Ffield, A., L.Gordon, A., & Adi, R. (2012). *Variability of Indonesian through flow within Makassar*.
20. J. Koto, A.Maimun, 2017, *Riser and Its Application on Oil and Gas Exploration-*, Third Edition, Ocean & Aerospace Research Institute, Indonesia.

JAse | Received: 25-July-2018 | Accepted: 30-August-2018 | [(15) 1: 1-9]
Published by International Society of Ocean, Mechanical and Aerospace Scientists and Engineers, www.isomase.org., ISSN: 2442-6407